Supramolecular Chemistry
Publication details, including instructions for authors and subscription information:
http://www.informaworld.com/smpp/title~content=t713649759

Lanthanide-Organic Frameworks with Flexible Triacid Ligand: Structural Variation Under Different Reaction Conditions

Zheng-Hua Zhang[a]; Wen-Li[a]; Taka-Aki Okamura[b]; Ling-Yan Kong[a]; Wei-Yin Sun[a]; Norikazu Ueyama[b]
[a] Coordination Chemistry Institute, State Key Laboratory of Coordination Chemistry, Nanjing University, Nanjing, P.R. China [b] Department of Macromolecular Science, Graduate School of Science, Osaka University, Toyonaka, Osaka, Japan

To cite this Article Zhang, Zheng-Hua , Wen-Li, Okamura, Taka-Aki , Kong, Ling-Yan , Sun, Wei-Yin and Ueyama, Norikazu(2006) 'Lanthanide-Organic Frameworks with Flexible Triacid Ligand: Structural Variation Under Different Reaction Conditions', Supramolecular Chemistry, 18: 4, 317 — 325
To link to this Article: DOI: 10.1080/10610270600584080
URL: http://dx.doi.org/10.1080/10610270600584080

Supramolecular Chemistry, June 2006 Vol. 18 (4), pp. 317–325

Taylor & Francis
Taylor & Francis Group

Lanthanide-Organic Frameworks with Flexible Triacid Ligand: Structural Variation Under Different Reaction Conditions

ZHENG-HUA ZHANG[a], WEN-LI MENG[a], TAKA-AKI OKAMURA[b], LING-YAN KONG[a], WEI-YIN SUN[a,*] and NORIKAZU UEYAMA[b]

[a]*Coordination Chemistry Institute, State Key Laboratory of Coordination Chemistry, Nanjing University, Nanjing 210093, P.R. China;* [b]*Department of Macromolecular Science, Graduate School of Science, Osaka University, Toyonaka, Osaka 560-0043, Japan*

Received 10 October 2005; Accepted 16 January 2006

Three metal-organic frameworks (MOFs) $[La(bta)(H_2O)]_n$ (1), $[La(bta)(H_2O)_2{\cdot}H_2O]_n$ (2) and $[Er(bta)(H_2O)_2{\cdot}H_2O]_n$ (3) with different structures were synthesized by reactions of 1,3,5-benzenetriacetic acid (H_3bta) with the corresponding lanthanide salts under different conditions. X-ray diffraction analyses reveal that complexes 1 and 2 have the same metal atom and ligand but different structures. In 1, each bta^{3-} adopts *cis*, *cis*, *cis* conformation and acts as a μ_6-bridge linking six lanthanum atoms to form a 2D framework; while in 2, the bta^{3-} has *cis*, *trans*, *trans* conformation and serves as a μ_5-bridging ligand, which results in a 3D channel-like structure. In the case of 3, each bta^{3-} also adopts *cis*, *trans*, *trans* conformation but acts as a μ_4-bridge linking four erbium atoms to form a 3D channel-like framework. The results imply that the reaction conditions have great impact on the structure of MOFs, and the flexible triacid ligand H_3bta is versatile and can adopt different conformations in the formation of MOFs. The magnetic property of complex 3 was investigated in the temperature range of 1.8–300 K.

Keywords: Lanthanide; Metal-organic frameworks; Crystal structures; Magnetic properties

INTRODUCTION

The construction of metal-organic frameworks (MOFs) is a rapid growth field in supramolecular chemistry due to their unusual topologies and potential applications [1–5]. The studies reported to now show that the nature of organic ligands and the coordination requirements of metal ions play crucial rules in construction of MOFs. As a result, a variety of organic ligands with different coordination groups were designed and prepared in the past years. Among these reported ligands, carboxylate-containing ligands have been widely used in construction of MOFs containing transition metal ions because of the varied binding modes of the carboxylate group [6–11]. However, the most of the used carboxylate-containing ligands e.g., 1,3,5-benzenetricarboxylic acid, 1,4-benzenedicarboxylic acid (*p*-H_2BDC) and 1,3-benzenedicarboxylic acid (*m*-H_2BDC), are rigid. The use of flexible carboxylate-containing ligands as building blocks in the construction of MOFs are not well carried out to now. In addition, the use of lanthanide salts for constructing MOFs has been a rapidly developing area in recent years due to the high coordination numbers as well as special properties of the lanthanide ions [12–14].

We are interested in the construction of MOFs with flexible organic ligands owing to their flexibility and conformational freedoms. In our previous studies, we obtained various MOFs with specific structures and interesting properties by using imidazole-containing ligands such as 1,3,5-tris(1-imidazolyl)-2,4,6-trimethylbenzene (titmb) [15–19]. This is a flexible ligand since there are methylene groups between the central aromatic core and the coordinating imidazole groups. The results demonstrated that titmb could adopt different conformations when it interacts with metal ions. In this paper, we report three MOFs $[La(bta)(H_2O)]_n$ (**1**), $[La(bta)(H_2O)_2{\cdot}H_2O]_n$ (**2**) and $[Er(bta)(H_2O)_2{\cdot}H_2O]_n$ (**3**) by using flexible

*Corresponding author. Fax: +86-25-83314502. E-mail: sunwy@nju.edu.cn

ISSN 1061-0278 print/ISSN 1029-0478 online
DOI: 10.1080/10610270600584080

ligand 1,3,5-benzenetriacetic acid (H_3bta) and corresponding lanthanide salts under different conditions, which may provide a useful strategy to synthesize new MOFs.

EXPERIMENTAL

All commercially available chemicals are of reagent grade and used as received without further purification. H_3bta ligand was obtained by the method described in the literature [20]. Hydrated lanthanide salts were prepared from the corresponding oxides according to literature methods [21]. C, H and N analyses were made on a Perkin-Elmer 240C elemental analyzer at the analysis center of Nanjing University. Infrared (IR) spectra were recorded on a Bruker Vector22 FT-IR spectrophotometer by using KBr discs. Thermogravimetric and differential thermal analyses were performed on a simultaneous SDT 2960 thermal analyzer. Powder samples were loaded into alumina pans and heated under N_2 at a heating rate of 10°C/min. The temperature-dependent magnetic susceptibilities in the temperature range of 1.8–300 K under a constant external magnetic field of 2000 G were performed on an MPMS-SQUID magnetometer. The diamagnetic contributions of the samples were corrected by using Pascal's constants.

Preparation of $[La(bta)(H_2O)]_n$ (1)

A mixture of H_3bta (37.8 mg, 0.15 mmol), $La(NO_3)_3{\cdot}6H_2O$ (21.7 mg, 0.05 mmol), $FeCl_3$ (12.2 mg, 0.075 mmol), C_2H_5OH (2 mL) and H_2O (12 mL) was kept in a Teflon liner autoclave at 160 °C for 3 days. After the mixture was cooled to room temperature, yellow platelet crystals were collected with a yield of 30%. Anal. Cacld for $C_{12}H_{11}LaO_7$: C, 35.49; H, 2.73. Found: C, 35.51; H, 2.79%. IR (KBr, cm^{-1}): 3385 (br), 1599 (s), 1537 (vs), 1458 (m), 1434 (s), 1405 (s), 1283 (m), 1261 (m), 1160 (m), 954 (m), 811 (m), 694 (m), 684 (m).

Preparation of $[La(bta)(H_2O)_2{\cdot}H_2O]_n$ (2)

The solvothermal reaction of $La(NO_3)_3{\cdot}6H_2O$ (21.7 mg, 0.05 mmol), ZnO (16.3 mg, 0.15 mmol), H_3bta (25.2 mg, 0.1 mmol), H_2O (12 mL) and C_2H_5OH (2 mL) at 160°C for 3 days led to the formation of colorless crystals of complex **2**. Yield: 50%. Anal. Cacld for $C_{12}H_{15}LaO_9$: C, 32.60; H, 3.42. Found: C, 32.69; H, 3.37%. IR (KBr, cm^{-1}): 3406 (br), 1637 (m), 1604 (m), 1542 (vs), 1446 (s), 1411 (vs), 1304 (m), 1282 (w), 1174 (m), 944 (w), 816 (m), 696 (m), 643 (m).

Preparation of $[Er(bta)(H_2O)_2{\cdot}H_2O]_n$ (3)

A mixture of $Er(NO_3)_3{\cdot}6H_2O$ (46.1 mg, 0.1 mmol), H_3bta (50.4 mg, 0.2 mmol), $Ni(OH)_2$ (13.9 mg, 0.15 mmol) or $Cu_2CO_3(OH)_2{\cdot}2H_2O$ (19.3 mg, 0.075 mmol) and H_2O (14 mL) was sealed in a stainless-steel vessel and placed in an oven at 175°C for 3 days. After cooling to room temperature during 12 hours, colorless block crystals of **3** were obtained. Yield: 50%. Anal. Calcd for $C_{12}H_{15}O_9Er$: C, 30.63; H, 3.21%. Found: C, 30.65; H, 3.13%. IR (KBr, cm^{-1}): 3501 (s), 3258 (br), 1651 (m), 1572 (vs), 1553 (vs), 1452 (vs), 1431 (vs), 1410 (vs), 1318 (s), 1282 (m), 1245 (s), 1194 (m), 1159 (m), 952 (w), 810 (m), 752 (m), 679 (m).

Crystallography

The data collection for **1**–**3** was carried on a Rigaku RAXIS-RAPID Imaging Plate diffractometer using graphite-monochromated Mo-Kα radiation (λ = 0.7107 Å). The structures were solved by direct

TABLE I Crystallographic data for complexes **1**–**3**

Complex	**1**	**2**	**3**
Formula	$C_{12}H_{11}O_7La$	$C_{12}H_{15}O_9La$	$C_{12}H_{15}O_9Er$
Formula weight	406.12	442.15	470.50
Crystal system	monoclinic	triclinic	monoclinic
Space group	*C* 2/m	*P*-1	$P2_1/n$
a, Å	8.388(5)	8.722(5)	10.757(4)
b, Å	15.193(7)	9.258(5)	8.388(3)
c, Å	9.716(5)	9.854(5)	16.108(7)
α, °	90.00	112.601(16)	90.00
β, °	101.496(16)	97.345(16)	105.838(13)
γ, °	90.00	95.024(18)	90.00
V, Å^3	1213.3(10)	720.4(7)	1398.2(10)
Z	4	2	4
D_c (g cm^{-3})	2.223	2.038	2.235
μ, cm^{-1}	35.52	30.09	60.48
Reflections collected	5981	7113	13155
Unique reflections	1441	3251	3192
R_{int}	0.0484	0.0412	0.0341
*R*1[I > 2σ(I)]	0.0219	0.0257	0.0169
*wR*2[I > 2σ(I)]	0.0309[a]	0.0367[b]	0.0279[c]

[a] $w = 1/[\sigma^2(F_o^2) + (0.0010P)^2 + 0.0000P]$. [b] $w = 1/[\sigma^2(F_o^2) + (0.0000P)^2 + 0.0000P]$. [c] $w = 1/[\sigma^2(F_o^2) + (0.0090P)^2 + 0.0000P]$.

methods with SIR92 [22]. All non-hydrogen atoms were refined anisotropically by the full-matrix least-square method [23]. The hydrogen atoms were placed in calculated positions of idealized geometry. All calculations were carried out on SGI workstation using the teXsan crystallographic software package of Molecular Structure Corporation [24]. Details of the crystal parameters, data collection and refinements are summarized in Table I, and selected bond lengths and angles with their estimated standard deviations are listed in Table II. Crystallographic data (excluding structure factors) for the structures reported in this paper have been deposited with the Cambridge Crystallographic Data Center as supplementary publication No. CCDC-278838 (**1**), CCDC-278839 (**2**) and CCDC-278840 (**3**). Copies of the data can be obtained free of charge on application to CCDC, 12 Union Road, Cambridge CB2 1EZ, UK (fax: +44-1221-336-003; e-mail: deposit@ccdc.cam.ac.uk).

RESULTS AND DISCUSSION

Description of Crystal Structures

Complex [La(bta)(H$_2$O)]$_n$ (1)

The single-crystal X-ray analysis revealed that the complex **1** crystallizes in space group C2/m with only the lanthanide metal atom centers, without the Fe(III) ions. As shown in Fig. 1a, the La(III) center is coordinated by nine oxygen atoms, in which eight from six bta^{3-} ligands and one (O4) from a

TABLE II Selected bond distances (å) and angles (°) for complexes **1**–**3**

[La(bta)(H$_2$O)]$_n$ (**1**)					
La-O1	2.553(2)	La-O1^{i}	2.553(2)	La-O2	2.665(2)
La-O2^{i}	2.665(2)	La-O2^{ii}	2.583(2)	La-O2^{iii}	2.583(2)
La-O3	2.4775(19)	La-O3^{i}	2.4775(19)	La-O4	2.519(3)
O1-La-O1^{i}	155.24(8)	O1-La-O2	49.74(6)	O1-La-O2^{i}	135.90(6)
O1-La-O2^{ii}	75.74(6)	O1-La-O2^{iii}	114.27(6)	O1-La-O3	80.32(6)
O1-La-O3^{i}	80.09(6)	O1-La-O4	102.38(4)	O1^{i}-La-O2	135.90(6)
O1^{i}-La-O2^{i}	49.74(6)	O1^{i}-La-O2^{ii}	114.27(6)	O1^{i}-La-O2^{iii}	75.74(6)
O1^{i}-La-O3	80.09(6)	O1^{i}-La-O3i	80.32(6)	O1^{i}-La-O4	102.38(4)
O2-La-O2^{i}	160.70(7)	O2-La-O2^{ii}	107.38(6)	O2-La-O2^{iii}	64.69(7)
O2-La-O3	73.21(6)	O2-La-O3^{i}	123.71(6)	O2-La-O4	80.35(4)
O2^{i}-La-O2^{ii}	64.69(7)	O2^{i}-La-O2^{iii}	107.38(6)	O2^{i}-La-O3	123.71(6)
O2^{i}-La-O3^{i}	73.21(6)	O2^{i}-La-O4	80.35(4)	O2^{ii}-La-O2^{iii}	134.80(8)
O2^{ii}-La-O3^{i}	145.97(6)	O2^{ii}-La-O3i	77.36(6)	O2 -La-O4	67.40(4)
O2^{iii}-La-O3	77.36(6)	O2^{iii}-La-O3^{i}	145.97(6)	O2^{iii}-La-O4	67.40(4)
O3-La-O3^{i}	74.96(9)	O3-La-O4	142.52(5)	O3^{i}-La-O4	142.52(5)
[La(bta)(H$_2$O)$_2$·H$_2$O]$_n$ (**2**)					
La-O1	2.524(3)	La-O1^{iv}	2.819(3)	La-O2^{iv}	2.557(3)
La-O3	2.608(2)	La-O4	2.610(2)	La-O5	2.547(2)
La-O6^{v}	2.498(2)	La-O7	2.5403	La-O8	2.602(2)
O1-La-O1^{iv}	62.44(10)	O1-La-O2^{iv}	110.18(9)	O1-La-O3	78.40(8)
O1-La-O4	72.99(7)	O1-La-O5	78.54(8)	O1-La-O6^{v}	148.90(8)
O1-La-O7	139.88(7)	O1-La-O8	72.39(8)	O1^{iv}-La-O2^{iv}	47.75(7)
O1^{iv}-La-O3	114.61(7)	O1^{iv}-La-O4	68.56(7)	O1^{iv}-La-O5	134.70(7)
O1^{iv}-La-O6^{v}	118.74(7)	O1^{iv}-La-O7	109.99(8)	O1^{iv}-La-O8	74.06(7)
O2^{iv}-La-O3	126.19(7)	O2^{iv}-La-O4	80.58(8)	O2^{iv}-La-O5	156.82(7)
O2^{iv}-La-O6^{v}	77.45(8)	O2^{iv}-La-O7	74.83(9)	O2^{iv}-La-O8	89.05(8)
O3-La-O4	50.22(7)	O3-La-O5	75.98(8)	O3-La-O6^{v}	73.42(8)
O3-La-O7	132.27(8)	O3-La-O8	140.61(8)	O4-La-O5	122.55(8)
O4-La-O6^{v}	78.94(8)	O4-La-O7	144.41(7)	O4-La-O8	137.56(8)
O5-La-O6^{v}	106.55(8)	O5-La-O7	84.81(9)	O5-La-O8	72.82(8)
O6^{v}-La-O7	70.95(8)	O6^{v}-La-O8	138.70(9)	O7-La-O8	67.86(8)
[Er(bta)(H$_2$O)$_2$·H$_2$O]$_n$ (**3**)					
Er-O1	2.4307(18)	Er-O2	2.6183(19)	Er-O2^{iv}	2.3052(19)
Er-O3	2.3973(19)	Er-O4	2.3898(18)	Er-O5	2.3685(18)
Er-O6	2.4892(18)	Er-O7	2.3154(19)	Er-O8	2.3573(19)
O1-Er-O2	51.05(6)	O1-Er-O2^{iv}	118.38(6)	O1-Er-O3	146.03(6)
O1-Er-O4	143.68(6)	O1-Er-O5	82.48(6)	O1-Er-O6	70.85(6)
O1-Er-O7	78.36(7)	O1-Er-O8	79.63(6)	O2-Er-O2^{iv}	67.51(6)
O2-Er-O3	133.87(6)	O2-Er-O4	149.77(6)	O2-Er-O5	72.70(6)
O2-Er-O6	104.06(6)	O2-Er-O7	124.82(6)	O2-Er-O8	70.13(6)
O2^{iv}-Er-O3	80.84(6)	O2^{iv}-Er-O4	89.40(6)	O2^{iv}-Er-O5	75.09(6)
O2^{iv}-Er-O6	126.94(6)	O2^{iv}-Er-O7	156.05(6)	O2^{iv}-Er-O8	84.63(6)
O3-Er-O4	54.69(6)	O3-Er-O5	131.17(6)	O3-Er-O6	121.90(6)
O3-Er-O7	76.57(7)	O3-Er-O8	74.42(6)	O4-Er-O5	82.95(6)
O4-Er-O6	73.72(6)	O4-Er-O7	84.07(6)	O4-Er-O8	129.04(6)
O5-Er-O6	53.48(6)	O5-Er-O7	126.54(6)	O5-Er-O8	142.21(6)
O6-Er-O7	73.10(6)	O6-Er-O8	144.27(6)	O7-Er-O8	81.75(6)

Symmetry transformations used to generate equivalent atoms: (i) −x, −y, −z + 2; (ii) x − (1/2), −y + (1/2), z; (iii) −x + (1/2), −y + (1/2), −z + 2; (iv) −x + 1, −y + 1, −z; (v) x + 1, −y + 2, −z.

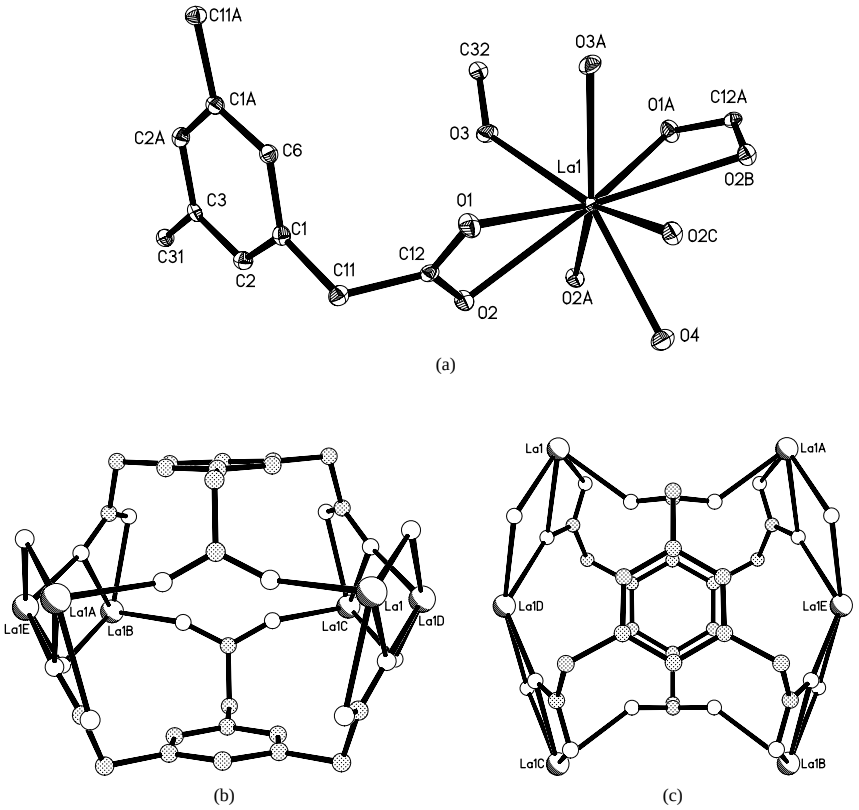

FIGURE 1 (a) ORTEP plot of 1 showing local coordination environment of La(III) with thermal ellipsoids at 30% probability. Side (b) and top (c) views of a capsule-like moiety in 1 formed by six La(III) atoms and two bta ligands. The hydrogen atoms were omitted for clarity.

coordinated water molecule. The La-O distances are in the range of 2.4775(19) to 2.665(2) Å, and the O-La-O bond angles vary from 49.74(6)° to 160.70(7)° (Table II). In this complex, each bta^{3-} ligand acts as a μ_6-bridge to link six lanthanum atoms as illustrated in Scheme 1a. Namely, one carboxylate group adopts a μ_2-η^1:η^1-bridging (each oxygen atom of the carboxylate connects one metal ion and the carboxylic group coordinates to two metal ions) coordination mode, while each of the other two carboxylate groups adopts a μ_2-η^2:η^1-bridging (one oxygen atom of the carboxylate connects two metal ions, the other one connects one metal ion, the carboxylic group coordinates to two metal ions) coordination mode. All bta^{3-} ligands in **1** adopt *cis*, *cis*, *cis* conformations and two bta^{3-} ligands take face-to-face orientation and link six La(III) atoms to form a capsule-like unit (Fig. 1b and 1c). In this capsule, the six metal atoms are completely coplanar while the two ligands lie up and down the La(III) plane, respectively. The two benzene ring planes are parallel each other with a centroid-centroid distance of 6.36 Å. Such capsule moieties are further connected by La-O bonds to form a 2D network structure (Fig. 2).

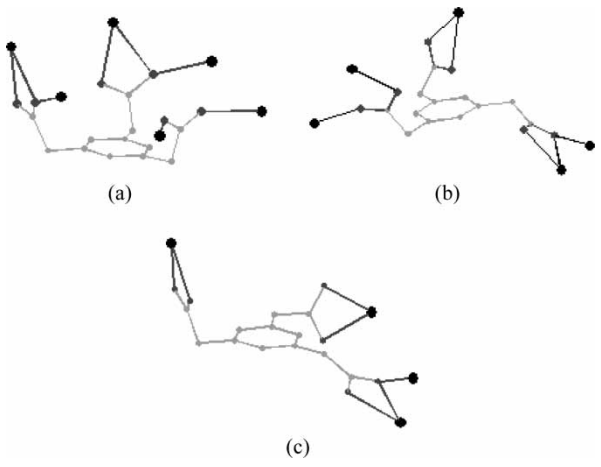

SCHEME 1 Conformation and coordination model of bta^{3-} ligand.

Complex [La(bta)(H$_2$O)$_2$·H$_2$O]$_n$ (2)

The crystallographic study demonstrates that complex **2** has the same metal/ligand ratio as that in **1**, namely there are also only lanthanide metal atom centers in **2**. However, the structure of **2** is entirely different from that of **1**. In complex **2**, the La(III) center is also coordinated by nine oxygen atoms, but seven of them are from five bta^{3-} ligands and the other two (O7 and O8) are from two coordinated water molecules (Fig. 3a). The La-O distances are in the range of 2.498(2) to 2.819(3) Å, and the O-La-O coordination angles vary from 47.75(7)° to 156.82(7)° (Table II). In contrast to the μ_6-bridging mode of bta^{3-} ligand in **1**, each bta^{3-} ligand serves as a μ_5-bridge to link five lanthanum atoms (Scheme 1b), in which one carboxylate group adopts a μ_1-η^1:η^1-chelating

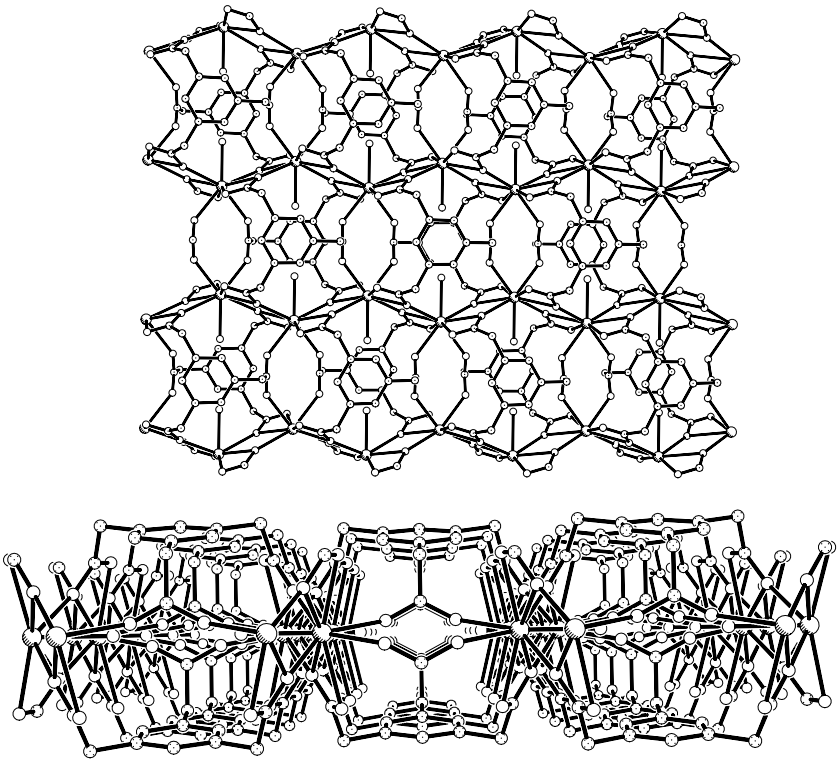

FIGURE 2 Top (upper) and side (down) views of 2D network structure of **1**, hydrogen atoms were omitted for clarity.

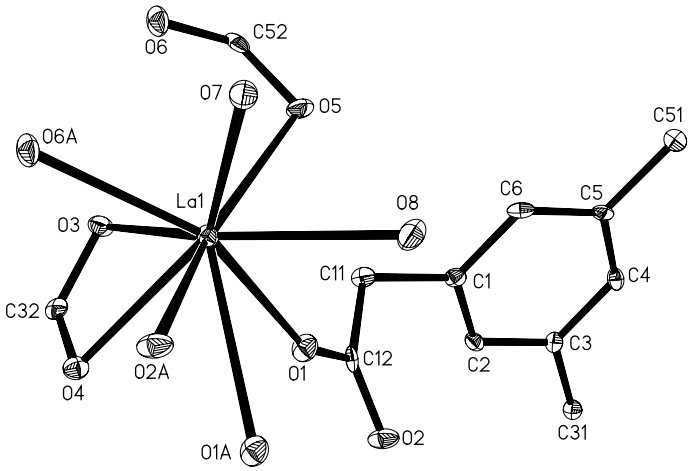

(a)

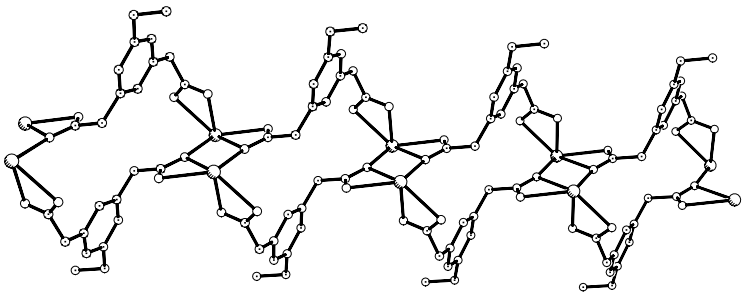

(b)

FIGURE 3 (a) ORTEP plot of 2 showing local coordination environment of La(III) with thermal ellipsoids at 30% probability. The hydrogen atoms were omitted for clarity. (b) 1D chain structure in **2**, hydrogen atoms were omitted for clarity.

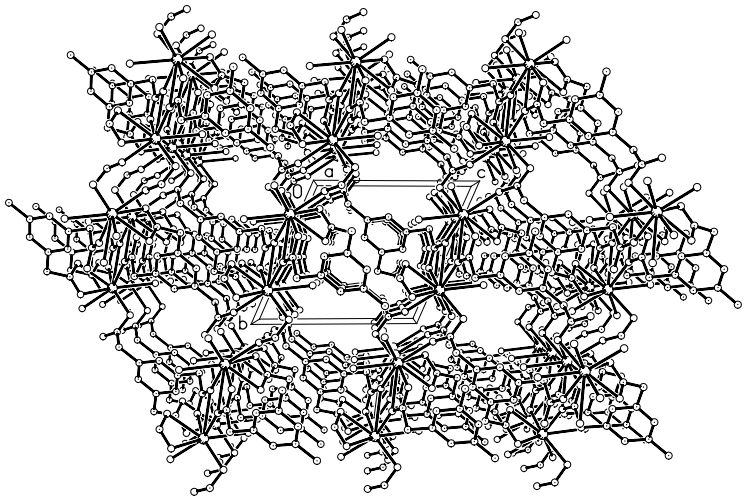

FIGURE 4 3D structure of **2** viewing along the *a* axis, guest water molecules are omitted for clarity.

(each oxygen atom of the carboxylate connects one metal ion and the carboxylic group coordinates to one metal ion) mode coordinating to one lanthanum atom, the second one adopts a μ_2-η^2:η^1-bridging coordination mode and the third one adopts a μ_2-η^1:η^1-bridging mode. If the linkage of the μ_2-η^1:η^1-bridging carboxylate groups in bta^{3-} are neglected, it can be found that two La(III) atoms and two bta^{3-} ligands (each bta^{3-} using two of the three pendant arms connects two La atoms) formed a 20-membered macrocyclic ring (20MR), and then the rings are connected by bridging carboxylate groups to form a 1D chain structure (Fig. 3b). In this chain, all bta^{3-} ligands have *cis*, *trans*, *trans* conformation and adopt back-to-back orientation with the benzene rings of bta^{3-} paralleling each other. Then the 1D chains are linked by the μ_2-η^1:η^1-bridging carboxylate groups to form a 3D channel-like structure (Fig. 4), and the uncoordinated water molecules are located in the channels (Fig. 5). There are four kinds of hydrogen bonds in **2**: (a) hydrogen bonding between the uncoordinated and coordinated water molecules with O···O distances of 2.718(17)–3.023(4) Å; (b) hydrogen bonding between the uncoordinated water molecules and the carboxylate oxygen atoms with O···O distances of 2.811(4) Å; (c) hydrogen bonding of coordinated water molecules with carboxylate oxygen atoms [O···O distances: 2.687(3)–2.745(3) Å]; and (d) hydrogen bonding of carboxylate oxygen atoms/methylene carbon atoms (C···O distances: 3.306–3.381 Å).

Complex $[Er(bta)(H_2O)_2{\cdot}H_2O]_n$ (3)

In complex **3**, the Er(III) center is also nine-coordinate, but in which seven oxygen atoms are from four bta^{3-} ligands and the other two are from two coordinated water molecules (Fig. 6). The Er-O

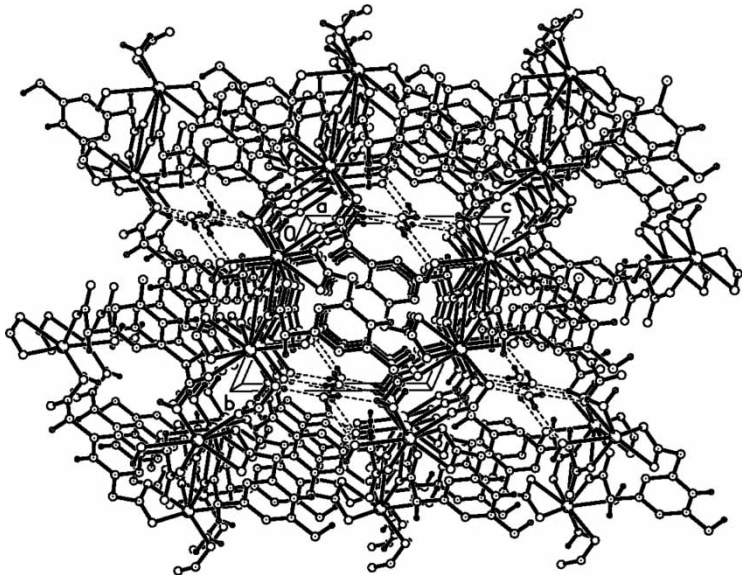

FIGURE 5 Packing structure along the *a* axis of **2** with guest water molecules, the hydrogen bonds were indicated by dashed lines.

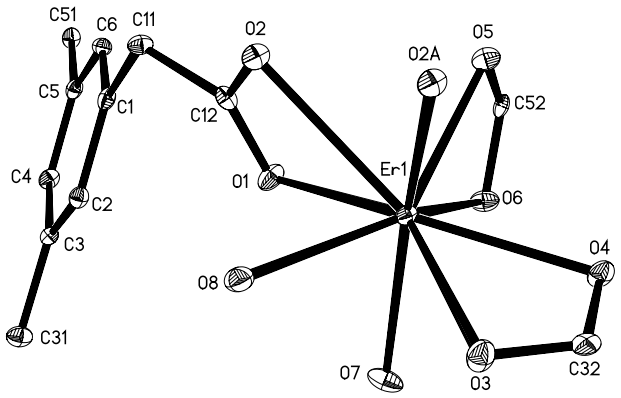

FIGURE 6 ORTEP plot of **3** showing local coordination environment of Er(III) with thermal ellipsoids at 30% probability.

distances range from 2.3052(19) to 2.6183(19)Å, and the O-Er-O angles vary from 51.05(6)° to 156.05(6)° (Table II). Very different from the above two La(III) complexes, each bta^{3-} ligand in **3** plays as a μ_4-bridge to join four metal atoms (Scheme 1c), that is, one carboxylate group adopts a μ_2-η^2:η^1-bridging coordination mode, while each of the other two carboxylate groups adopts a μ_1-η^1:η^1-chelating mode. If the bridging roles of O2 atoms (see Fig. 6) are neglected, it could be found that each bta^{3-} ligand adopts *cis*, *trans*, *trans* conformation to connect three Er(III) atoms and each Er(III) atom coordinates to three bta^{3-} ligands to form a 2D network (Fig. 7a), and the network looks like square-wave-like chains from the side view (Fig. 7b). Then the 2D networks are joined by bridging O2 atoms to form a 3D channel-like structure (Fig. 8), and the guest water molecules are located in the channels (Fig. 9). There are also abundant hydrogen bonds in **3**: (a) hydrogen bonding between the uncoordinated and coordinated water molecules with O···O distances of 2.679(3)–3.094(3) Å; (b) hydrogen bonding between the uncoordinated water molecules and the carboxylate oxygen atoms with O···O distances of 2.843(3)–2.891(3) Å; (c) hydrogen bonding of coordinated water molecules with carboxylate oxygen atoms [O···O distances: 2.647(3)–2.724(3) Å]; and (d) hydrogen bonding of uncoordinated water molecules/benzene ring carbon atoms [C···O distances: 3.468(3) Å].

From the results described above, it was found that the flexible bta^{3-} ligand can have *cis*, *trans*, *trans* and *cis*, *cis*, *cis* two different conformations, which is the same as the previously reported flexible imidzole-containing tripodal ligands [15–19]. Furthermore, the deprotonated carboxylate groups can further adopt different coordination modes when they interact with the metal atoms, for examples, μ_1-η^1:η^0-monodenate, μ_2-η^2:η^1-bridging, μ_3-η^2:η^2-bridging, μ_3-η^2:η^1-bridging, μ_2-η^1:η^1-bridging and μ_1-η^1:η^1-chelating coordination modes [25–28]. The results imply that the flexible tricarboxylate ligand is versatile and can adopt different conformation and coordination modes under different reaction conditions, which would leads to the formation of varied structures.

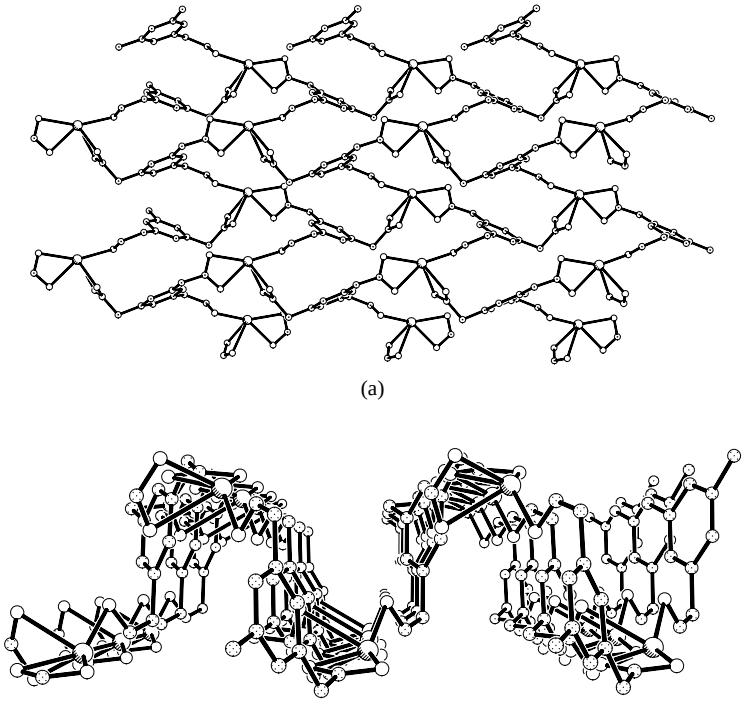

(a)

(b)

FIGURE 7 The 2D network structure in **3** from (a) top view and (b) side view.

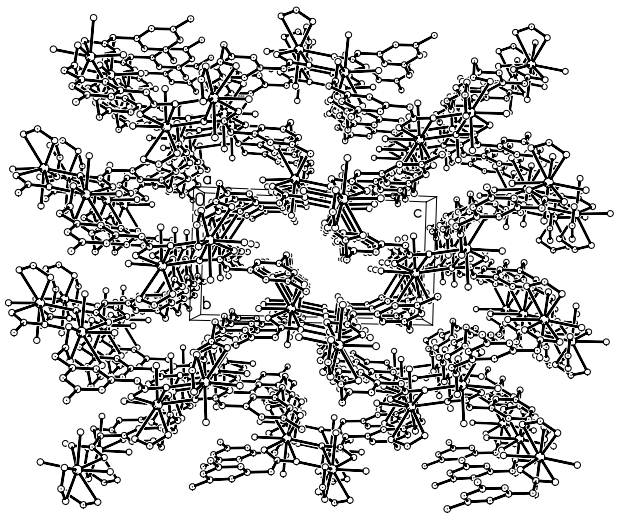

FIGURE 8 3D structure of **3** viewing along the *a* axis, guest water molecules are omitted for clarity.

In our previous studies, the reactions of the H_3bta ligand with only transition-metal salts or only lanthanide metal salts have been carried out, and complexes with different structures and properties were obtained [25–28]. In these complexes, we found that the most of the transition metal complexes are soluble but the lanthanide complexes are almost insoluble in water and common organic solvents. Then, in order to investigate the MOFs with both lanthanide and transition metal centers, the H_3bta was used to react with lanthanide salts in the presence of transition metal salts and/or oxides under hydro(solvo)thermal conditions to give polymeric complexes. However, it is unexpected that in our experiments no heteronuclear complexes with both lanthanide and transition metal atoms were formed even in the presence of excess transition metal salts or oxides. Further experiments were attempted by layering method between the transition metal-bta complexes and the lanthanide salts, however the results showed that only the homonuclear lanthanide complexes were formed, which may be due to the difference of the solubility between lanthanide complexes and transition metal complexes as mentioned above, and the higher affinity of oxygen atoms to the lanthanide ions than to the transition metal ions. Nonetheless, the different structures of **1** and **2**, as well as the previously reported lanthanide-bta complexes indicate that the reaction conditions have great impact on the structure of MOFs. When the H_3bta reacted with $LaCl_3{\cdot}6H_2O$ without addition of any transition metal salts or oxides, complex $[La(bta)(H_2O)_2{\cdot}4.5H_2O]_n$ with different structure was obtained [27]. Such structural differences indicate that the addition of transition metal could tune the self-assembly product greatly, and this could provide a useful strategy for the synthesis of new MOFs.

Thermogravimetric Analyses (TGA) of the Complexes

Thermogravimetric analyses (TGA) were performed on crystalline samples of these complexes in the range of 20–800 °C under nitrogen atmosphere. The TGA data for **1** show that no weight loss was observed for the complex until 300°C and then began to lose the coordinated water molecule and completed at 400 °C (the weight loss of $H_2O/[La(bta)(H_2O)]$ was 4.27%, calculated: 4.43%); the second weight loss was observed at 470°C in which the decomposition of the complex started. TGA data of **2** display that the first weight loss of 12.10% from 60 to 170°C corresponds to the loss of all water molecules ($3H_2O/[La(bta)(H_2O)_2{\cdot}H_2O]$,

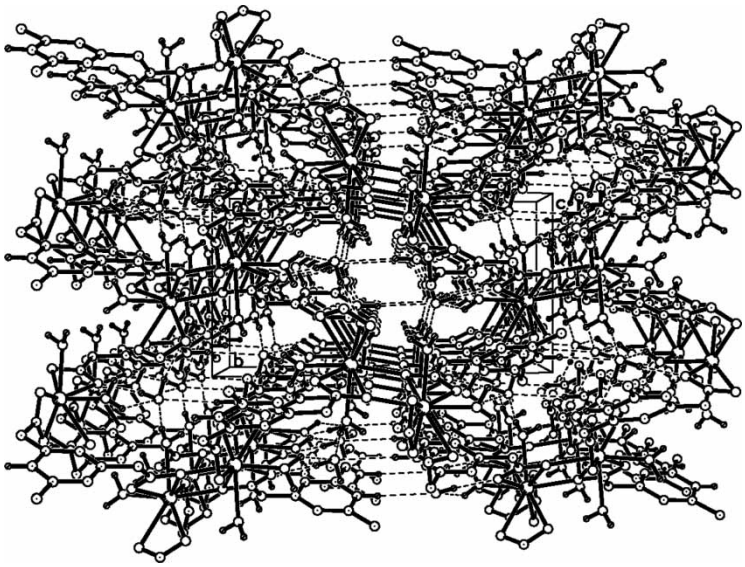

FIGURE 9 Packing diagram along the *a* axis of **3** with guest water molecules, the hydrogen bonds were indicated by dashed lines.

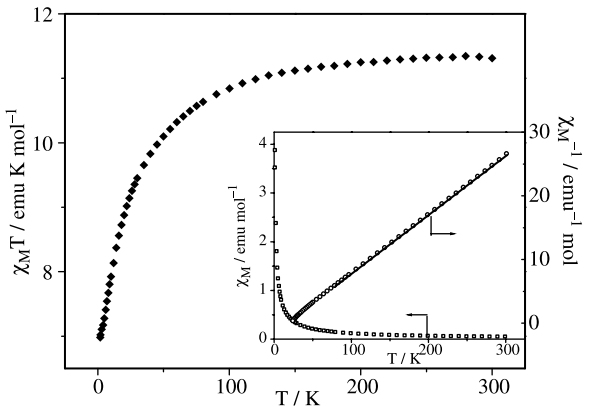

FIGURE 10 Temperature dependence of the $\chi_M T$ (◆) values for complex 3. Inset: Temperature dependence of the χ_M (□) and χ_M^{-1} (○) values, the solid line represents the best fit of the curve.

calculated: 12.21%), the second weight loss began at 370°C where the decomposition of the residue started. Distinction between weight losses from the coordinated and uncoordinated water was not clearly demonstrated in TGA data. This non-distinctive behavior is also reported in literature [29]. The TGA data of **3** display that the first weight loss of 11.02% (calcd. 11.48%) from 85 to 235°C corresponds to the loss of all water molecules (including two uncoordinated water and three coordinated water molecules). Distinction between two kinds of water molecules was also not clear, and no further weight loss was observed over the temperature range of 235–380°C.

Magnetic Properties of Complexes

Complexes **1** and **2** are expected to be diamagnetic since La(III) ion has no unpaired electrons, so only the magnetic property of complex **3** was investigated.

Variable-temperature magnetic susceptibility measurement was performed on powder samples of complex **3** in the temperature range of 1.8–300 K. Figure 10 gives a plot of $\chi_M T$ vs T and χ_M vs T for complex **3**. The $\chi_M T$ value at room temperature is 11.31 emu K mol^{-1}, which is lower than the spin-only value 11.48 emu K mol^{-1} for Er(III) unit ($^4I_{15/2}$, $g = 1.2$), and $\chi_M T$ decreases gradually by cooling the sample and reaches 6.98 emu K mol^{-1} at 1.8 K. The χ_M value is 0.0377 emu mol^{-1} at 300 K. With the decrease of the temperature, the values of the χ_M increase over the whole region of 1.8–300 K. The plot of χ_M^{-1} vs. T over the temperature range 60–300 K obeys the Curie–Weiss law with $C =$ 11.64 emu K mol^{-1} and $\theta = -7.27$ K. The decrease of $\chi_M T$ and the negative value of θ are due primarily to the splitting of the ligand field of the Er(III) ion together with the possible weak antiferromagnetic coupling between the Er(III) ions, considering a possible interaction path through carboxylate bridges [28].

Acknowledgements

This work was supported by the National Natural Science Foundation of China (Grant No. 20231020) and the National Science Fund for Distinguished Young Scholars (Grant No. 20425101).

References

[1] Batten, S. R.; Robson, R. *Angew. Chem. Int. Ed.* **1998**, *37*, 1460.
[2] Paz, F. A. A.; Klinowski, J. *Chem. Commun.* **2003**, 1484.
[3] Kitagawa, S.; Kitaura, R.; Noro, S. *Angew. Chem. Int. Ed.* **2004**, *43*, 2334.
[4] Kitaura, R.; Fujimoto, K.; Noro, S.; Kondo, M.; Kitagawa, S. *Angew. Chem. Int. Ed.* **2002**, *41*, 133.
[5] Biradha, K.; Fujita, M. *Angew. Chem. Int. Ed.* **2002**, *41*, 3392.
[6] Cheng, D.; Khan, M. A.; Houser, R. P. *Inorg. Chem* **2001**, *40*, 6858.
[7] Choi, H. J.; Suh, M. P. *J. Am. Chem. Soc.* **1998**, *120*, 10622.
[8] Eddaoudi, M.; Kim, J.; Wachter, J. B.; Chae, H. K.; O'Keeffe, M.; Yaghi, O. M. *J. Am. Chem. Soc.* **2001**, *123*, 4368.
[9] Serre, C.; Millange, F.; Thouvenot, C.; Gardant, N.; Pell, F.; Férey, G. *J. Mater. Chem.* **2004**, *14*, 1540.
[10] Takamizawa, S.; Nakata, E.-i.; Saito, T. *Angew. Chem. Int. Ed.* **2004**, *43*, 1368.
[11] Kondo, M.; Irie, Y.; Shimizu, Y.; Miyazawa, M.; Kawaguchi, H.; Nakamura, A.; Naito, T.; Maeda, K.; Uchida, F. *Inorg. Chem.* **2004**, *43*, 6139.
[12] Pan, L.; Adams, K. M.; Hernandez, H. E.; Wang, X.; Zheng, C.; Hattori, Y.; Kaneko, K. *J. Am. Chem. Soc.* **2003**, *125*, 3062.
[13] Cao, R.; Sun, D. F.; Liang, Y. C.; Hong, M. C.; Kazuyuki, T.; Shi, Q. *Inorg. Chem.* **2002**, *41*, 2087.
[14] Kim, Y. J.; Suh, M.; Jung, D. Y. *Inorg. Chem.* **2004**, *43*, 245.
[15] Liu, H.-K.; Sun, W.-Y.; Tang, W.-X.; Yamamoto, T.; Ueyama, N. *Inorg. Chem.* **1999**, *38*, 6313.
[16] Sun, W.-Y.; Fan, J.; Okamura, T.-a.; Xie, J.; Yu, K.-B.; Ueyama, N. *Chem. Eur. J.* **2001**, *7*, 2557.
[17] Fan, J.; Sui, B.; Okamura, T.; Sun, W.-Y.; Tang, W.-X.; Ueyama, N. *J. Chem. Soc., Dalton Trans.* **2002**, 3868.
[18] Fan, J.; Zhu, H.-F.; Okamura, T.; Sun, W.-Y.; Tang, W.-X.; Ueyama, N. *Chem. Eur. J.* **2003**, *9*, 4724.
[19] Zhao, W.; Fan, J.; Okamura, T.; Sun, W.-Y.; Ueyama, N. *J. Solid State Chem.* **2004**, *177*, 2358.
[20] Newman, M. S.; Lowrie, H. S. *J. Am. Chem. Soc.* **1954**, *76*, 6196.
[21] Choppin, G. R.; Bünzli, J.-C. G. *Lanthanide Probes in Life, Chemical and Earth Sciences*; Elsevier: Amsterdam, 1989.
[22] SIR92: Altomare, A.; Cascarano, G.; Giacovazzo, C.; Guagliardi, A. *J. Appl. Cryst.* **1993**, *26*, 343.
[23] DIRDIF 94: Beurskens, P. T.; Admiraal, G.; Beurskens, G.; Bosman, W. P.; de Gelder, R.; Israel, R.; Smits, J. M. M. *The DIRDIF-94 program system, Technical Report of the Crystallography Laboratory*; University of Nijmegen: The Netherlands, 1994.
[24] teXsan: Crystal Structure Analysis Package, Molecular Structure Corporation, 1999.
[25] Zhu, H.-F.; Sun, W.-Y.; Okamura, T.-a.; Ueyama, N. *Inorg. Chem. Commun.* **2003**, *6*, 168.
[26] Zhu, H.-F.; Zhang, Z.-H.; Sun, W.-Y.; Okamura, T.-a.; Ueyama, N. *Cryst. Growth Des.* **2005**, *5*, 289.
[27] Zhang, Z.-H.; Shen, Z.-L.; Okamura, T.-a.; Zhu, H.-F.; Sun, W.-Y.; Ueyama, N. *Cryst. Growth Des.* **2005**, *5*, 1191.
[28] Zhang, Z.-H.; Okamura, T.-a.; Hasegawa, Y.; Kawaguchi, H.; Kong, L.-Y.; Sun, W.-Y.; Ueyama, N. *Inorg. Chem.* **2005**, *44*, 6219.
[29] Kim, Y. J.; Jung, D. Y. *Chem. Commun.* **2002**, 980.